DWR- 1622

150
11-17 e

MASTER

AEROSPACE
NUCLEAR
SAFETY

SC-PR-70-682

SANDIA LABORATORIES QUARTERLY REPORT
AEROSPACE NUCLEAR SAFETY PROGRAM
JULY 1 THROUGH SEPTEMBER 30, 1970

AEROSPACE NUCLEAR SAFETY DEPARTMENT 9510

Date Published - October 1970

SANDIA LABORATORIES

OPERATED FOR THE UNITED STATES ATOMIC ENERGY COMMISSION BY SANDIA CORPORATION | ALBUQUERQUE, NEW MEXICO, LIVERMORE, CALIFORNIA

P7506

DISCLAIMER

DISCLAIMER

Issued by Sandia Corporation,
a prime contractor to the United States Atomic Energy Commission

Available from the Clearinghouse,
U.S. Department of Commerce
Springfield, Va. 22151

Price: Paper Copy $3.00
Microfiche $0.65

SC-PR-70-682

SANDIA LABORATORIES QUARTERLY REPORT AEROSPACE NUCLEAR SAFETY PROGRAM JULY 1 THROUGH SEPTEMBER 30, 1970

Prepared by
Aerospace Nuclear Safety Department 9510
A. J. Clark, Jr., Manager

Sandia Laboratories
Albuquerque, New Mexico
87115

The cutoff date for information on this report was September 30, 1970

Compiled by
R. G. Illing, 9512

October 1970

ABSTRACT

This report describes research, development, support, and test activities in Sandia Laboratories Aerospace Nuclear Safety Program from July 1 through September 30, 1970.

Key words: SNAP-27, Pioneer, Brayton, DART

b

1-2

Blank Page

SUMMARY

SNAP-27

The delay in the Apollo 14 schedule has resulted in helium build-up in the SNAP-27 capsule; the reentry and Saturn V fireball/afterfire survival probabilities of the capsule are unchanged but the "margin of safety" will be diminished.

TRANSIT/PIONEER

The effect of edge radius on the Pioneer heat source terminal velocity was determined to be quite significant. A computer investigation of thermal stresses in the Pioneer heat shield is being conducted at Sandia to support and supplement the analytical effort of Isotopes. An aerodynamic model was prepared for the Pioneer heat source reentering crosswise, flat forward, unablated. Ortibal lifetimes were computed for the Pioneer heat source reentering alone after aborts corresponding to failure to ignite the TE 364 third stage.

ISOTOPE BRAYTON SYSTEM

An interim briefing for Mr. Klein, Director SNS, on the status of the Safety Feasibility Study was held July 22, 1970. A review of the preliminary rough draft report by the task force was held at Sandia August 25-27, 1970. A task force meeting will be held October 6-7, 1970, to review the revised draft report and a final briefing for Mr. Klein is scheduled for October 14, 1970.

ADVANCED FUELS SAFETY

Experiments demonstrated that long term alpha irradiation of molybdenum can produce changes that can be expected to alter the fracture properties of the molybdenum and could lead to dimensional changes. The new 40 kW hyperthermal arc was installed at Sandia.

FLINTNOSE-1

Ballistic parameters were determined for the five different heat sources on the FLINTNOSE-1 payload.

TABLE OF CONTENTS

RADIOISOTOPE SYSTEMS SAFETY SUPPORT

SAFETY TECHNOLOGY

TABLE OF CONTENTS
(continued)

RADIOISOTOPE SYSTEMS SAFETY SUPPORT

SNAP-27

Helium Pressures in the FCA-2 SNAP-27 Capsule
(C. J. M. Northrup, Jr.)

The FCA-2 SNAP-27 capsule is currently scheduled to be flown on the Apollo 14 mission. Since this mission has been delayed several times, a sufficient amount of helium will have been produced by launch time to alter the capsule's behavior in abort environments. The clad at the capsule midsection and the half capsule clad of the FCA-2 will open under internal gas pressures in the Earth-orbital decay (lateral spin), Earth-orbital decay (oriented), and superorbital (oriented) reentries. The graphite heat shield, however, should not be affected; therefore, the reentry survival probability of the SNAP-27 is unchanged. The clad at the capsule midsection and the half capsule clad will fail earlier in the Saturn V fireball/afterfire. The superorbital (lateral-spin) reentry will not cause the FCA-2 to depressurize. In all of the above situations, the capsule clad failures are a result of the FCA-2 capsule's storage period exceeding the SAR storage time limit, resulting in an increase in the helium pressure.

During normal operation, the helium pressure in the FCA-2 capsule while in the GLFC will be approximately 700 psi. This pressure produces a half capsule hoop stress of 11,900 psi and a longitudinal stress of 17,500 psi at the capsule midsection. The SNAP-27 capsule can easily accommodate these pressures for considerable lengths of time at normal operating temperatures. Even if an astronaut tugs on the flight handling tool (a 30 lb force can produce stresses as high as an additional 5500 psi), the FCA-2 capsule will not be affected as long as the clad temperature has not increased significantly above normal operating temperatures.

Because Haynes-25 loses its strength rapidly with increasing temperature, particular caution should be taken to avoid raising the temperature of the clad both before and after launch (for example--loss of on-pad-cooling, or the possibility of the astronaut dropping the heat source on the moon with a resultant partial burial situation). With the quantity of helium to be expected in the FCA-2 at the current Apollo 14 launch time, the midsection will fail if the clad is raised to approximately 1800°F (normal clad temperature in the LM is 1300°F).

The FCA-5 capsule is scheduled to be flown on the Apollo 15 in July, 1971, and the FCA-7 on the Apollo 16 during the winter of 1971-72. These capsules will be approximately the same age as the FCA-2 when they are flown; hence, difficulties similar to those experienced with the FCA-2 also may be expected with the two succeeding capsules.

The FCA-2, 5, and 7 SNAP-27 capsules can perform according to their original design specifications if the current Apollo schedules are kept. This results primarily from the capsules having been kept cool and not having used a significant amount of their creep lifetime. However, the "margin of safety" will be diminished, indicating particular care must be taken to prevent overheating of the capsules both before and after launch.

It should be noted that if the capsules are depressurized to one atmosphere of helium at 200°F shortly before launch, the capsule would then be predicted to survive a launch abort fireball from the standpoint of pressure failure. In addition, the margin of safety during reentry would be improved.

TRANSIT/PIONEER

Transit Reentry Verification Tests (D. E. Randall)

Four Transit heat sources were subjected to an orbital decay reentry heat load in the NASA/MSC 10 MW arcjet facility. A fifth test specimen was subjected to a thermal shock test condition by inserting it cold into the peak orbital decay reference heating rate for a 60-second run. All heat sources survived the test conditions. The test data are being analyzed by comparing them with analytical model behavior under the same test conditions.

In conjunction with the above tests, a Sandia-built calorimeter model in the Transit configuration was supplied to NASA/MSC for evaluation of heating rate distributions in the 10 MW arcjet facility. This model was instrumented with ten slug calorimeters to provide local heating rates for each of the three test conditions used for the Transit reentry heating rate simulation.

Postimpact Data (D. J. Sasmor)

Seven capsules from the Transit/Pioneer tests series conducted at Sandia Laboratories were sent to Los Alamos Scientific Laboratory for disassembly and fuel fines determinations. Prior to shipment, the tested capsules were leak checked, and the weight and volume were measured (Table I).

TABLE I

Results of Leak Tests of Impacted Transit/Pioneer Capsules

Capsule ID	Test	Leak	Wt(g)	Volume (cm^3 ±5)
T-23	Fragment Impact (Ignitor Assembly)	None detected	--	370
T-17	Fragment Impact (Electronic Package)	None detected	3892	370
T-34	Impact, 45° 2400°F, 325 fps (Nominal)	Leak at "Star" in Pt/Rh	3938	480
T-35	Impact, 22½° 2400°F, 325 fps (Nominal)	Leak at "Star" in Pt/Rh	3913	437
T-28	Impact, "End-on" 2400°F, 325 fps (Nominal)	2 small leaks in the Pt/Rh weld	3865	366
T-26	Impact, 45° 2000°F, 325 fps (Nominal)	Breached	--	364
P-10	Impact, "End-on" 2400°F, 325 fps (Nominal)	Leak at "Star" in Pt/Rh	3214	308

Rounding Effect on Terminal Velocity (A. C. Bustamante)

The effect of edge radius on the Pioneer heat source terminal velocity was determined. The effect of edge radius on terminal velocity was established and, as shown in Figure 1, is quite significant.

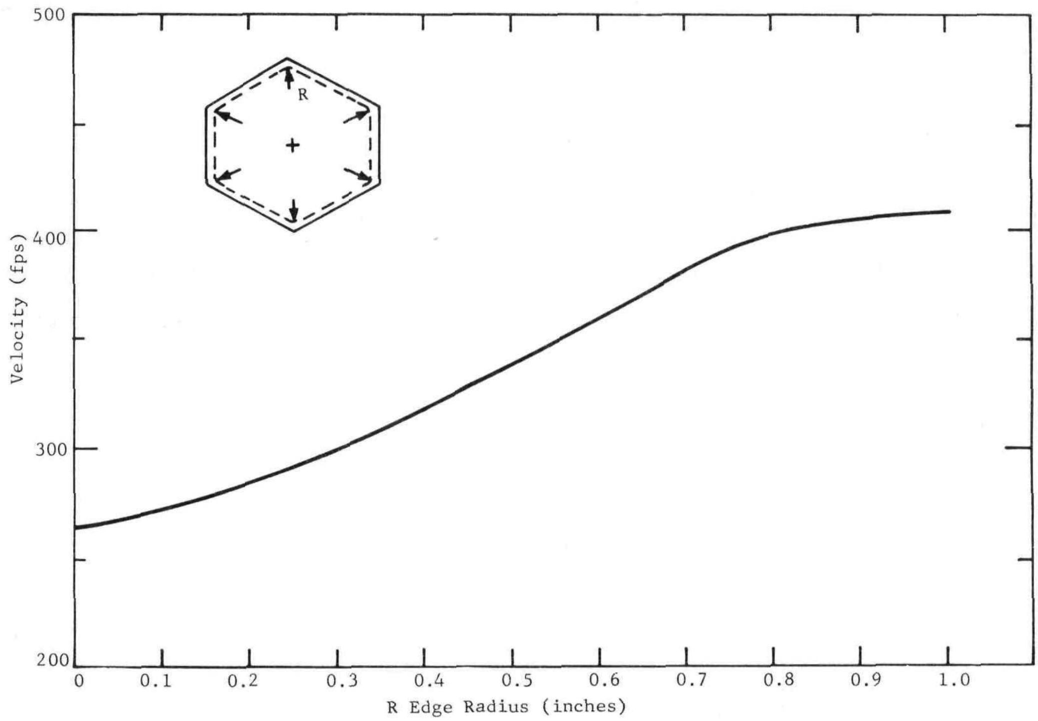

Figure 1. Effect of edge radius (rounding) on Pioneer heat source terminal velocity

Thermal Stresses (R. E. D. Stewart)

A computer investigation of thermal stresses in the Pioneer heat shield is being conducted at Sandia to support and supplement the analytical effort of Isotopes. In order to achieve the mathematical tractability required for analytical solutions, Isotopes' mathematical model replaces the actual heat shield geometry by an infinitely long (i.e., end effects are neglected) hollow circular cylinder whose OD is equal to the diameter of the largest circle which can be inscribed within the hexagonal outer profile of the heat shield. The analysis further assumes a state of plane strain and a material which is linearly elastic to the point of failure, and the variation of material properties with temperature is only approximately accounted for.

Since there are no known completely general three-dimensional stress codes operational, computer analysis will be subject to certain limitations. The Sandia computer codes being used, SAAS II and ARBAS H, are limited to axisymmetric, bi-linearly elastic solids of revolution with orthotropic temperature-dependent material properties subjected to axisymmetric thermal and/or mechanical loading. These same codes will handle asymmetric geometry and/or loading only in the case of two-dimensional problems such as plane stress or plane strain. In spite of these limitations, the computer analysis is expected to provide: (1) additional insight into the general nature of the stress distributions in the heat shield resulting from certain reentry or abort situations, (2) an indication of the significance of the errors introduced by assuming plane strain and neglecting end effects, and (3) an indication of the significance of the errors introduced by replacing the actual heat shield cross-section by that of the inscribed hollow circular cylinder.

To date, finite element meshes suitable for computer calculation of thermal stresses have been generated using program MESH. Since a much finer mesh is required for stress analysis than for thermal analysis a linear interpolation subroutine was added to the two-dimensional and three-dimensional thermal codes in order to provide the finer mesh of temperatures needed for input to the thermal stress codes. Initial results of the computer thermal stress analysis are expected soon.

Safety Tests (R. C. Cranfill)

Three Pioneer heat sources were impact tested at the Sandia Track facility. The test conditions are listed below:

Unit No.	Impact Attitude*	Velocity (ft/sec)	Temp (°F)
P-10	0°-End-On	325	2400
P-11	22½°	325	2400
P-8	45°	324	2400

*Impact attitude is defined as the angle between the velocity vector of the granite target and the longitudinal axis of the heat source.

Posttest examination of capsules indicated the 0° or end-on unit to be intact. This unit was sent to LASL for fuel simulant analyses. Units P-11 and P-8 had cracks in the primary impact area. No detectable fuel simulant was released from these capsules.

NASA/Langley Aeroheating Test Data (R. D. Klett)

Data from the Langley Pioneer aeroheating tests were corrected for adiabatic wall temperature and were averaged for use in two-dimensional heat transfer programs. For the unablated configuration, side-on-stable with flat forward, the side surfaces average heating rates from the Langley tests are 17 percent higher than the heating rates previously used by Sandia. The higher average rate is primarily caused by the high rates in the flow reattachment area. The Langley average heating rates to the side-on-stable, flat forward ablated configuration are 26 percent higher than those used in previous computations. Most of this increase is in the forward flat.

Effects of Mass Injecting, Chemical Reaction, and Hot Wall Correction on Aeroheating (R. D. Klett)

A study was conducted to determine the effects of mass injection into the boundary layer, surface oxidation, and the hot wall correction factor on the aerodynamic heating of a cross flow stable, flat forward, Pioneer heat source during orbital decay. Aeroheating rates from the NASA/Langley tests were used in conjunction with the Charring Material Ablation computer program to obtain the following results.

1. Since the CMA program assumes diffusion controlled ablation in the kinetic controlled regime, the net heating rates computed by CMA in free molecule flow (where pressures and surface temperatures are low) are not valid. Hot wall corrections can be used during free molecule flow.

2. Cold wall heating rates are 2 percent high in free molecule flow, 10 to 12 percent high at peak heating, 17 to 25 percent high near the end of the heat pulse, and 1.4 to 5.5 Btu/ft^2-sec low from the end of the heat pulse to earth impact. The percent error in cold wall heating rates increases with increasing heating ratios.

3. Heating rates corrected for hot wall only are less than 3 percent lower than net heating for the first part of the trajectory. After heating rates reach approximately 75 percent of peak, the errors in hot wall corrected rates increase. Hot wall rates are 4 to 7 percent low at peak heating and 18 to 27 percent low near the end of the heat pulse. After the heat pulse, hot wall rates vary from -2.9 to -11.4 Btu/ft^2-sec, but net heating is between 1.4 to 5.4 Btu/ft^2-sec because of surface oxidation.

4. Since neither cold wall nor hot wall corrected heating rates are sufficiently accurate, ablation analyses will be required for Pioneer orbital decay studies.

5. The surface impact temperatures of the Pioneer are near the transition between kinetic and diffusion controlled ablation. Conservative impact temperatures will be predicted by assuming the higher oxidation rates of diffusion controlled ablation all the way to impact.

These conclusions apply only to the Pioneer heat source during orbital decay and cannot be applied to other vehicles or other trajectories. Net heating rates from this study are being used in the Pioneer/Hittman thermal switch reentry analysis.

Aerodynamic and Trajectory Analyses (H. R. Spahr)

An aerodynamic model was prepared for the Pioneer heat source reentering crosswise, flat forward, unablated. The free-molecule hypersonic ballistic coefficient, based on free-molecule theoretical calculations, is 26.8 pounds per square foot. The continuum flow hypersonic ballistic coefficient, based on the NASA/Ames test data, is 50.6 pounds per square foot. Computer code HRS015 was used to compute the hypersonic ballistic coefficient in the transition flow regime. The subsonic ballistic coefficient, as measured by drop tests, is 71.3 pounds per square foot.

An orbital inclination of 31.4 degrees was selected for all orbital decay trajectory analyses. This orbital inclination corresponds to the mean orbital inclination of the launch vehicle when it is at velocities between circular and parabolic for the nominal trajectories in the General Dynamics phase I data package. Computer code HRS004 was used to compute the initial trajectory conditions for an orbital decay trajectory with this orbital inclination.

The TTB trajectory code was used to compute a Pioneer heat source orbital decay trajectory using the above aerodynamic data and initial conditions. The maximum reference heating rate for this trajectory is 127 Btu/ft^2-sec.

An aerodynamic model was also developed for the Pioneer heat source, reentering in a randomly tumbling mode. Computer code HRS015 was used to compute the hypersonic ballistic coefficient in the transition flow regime. The free molecule hypersonic ballistic coefficient is 41.2 pounds per square foot, and the continuum hypersonic ballistic coefficient is 62.0 pounds per square foot.

Orbital Lifetimes (H. R. Spahr)

Orbital lifetimes were computed for the Pioneer heat source reentering alone after aborts corresponding to failure to ignite the TE 364 third stage (i.e., same trajectory as aborts at Centaur MECO). For the resultant orbit, the computer code results, using nominal atmospheric data, are:

Pioneer heat source randomly tumbling
$\approx$27.8 years (most realistic value)

Pioneer heat source crosswise
$\approx$18.1 years (minimum value)

Pioneer heat source end-on
$\approx$47.2 years (maximum value)

Similar orbital lifetime calculations for the same abort were made for the Pioneer spacecraft and the Pioneer spacecraft with TE 364 motor (unburned). The results are:

Pioneer spacecraft, booms folded, randomly tumbling
$\approx$4.3 years (most realistic value)

Pioneer spacecraft, booms folded, end-on
$\approx$2.7 years (minimum value)

Pioneer spacecraft, booms folded, crosswise
$\approx$5.9 years (maximum value)

Pioneer spacecraft with unburned TE 364, booms folded, randomly tumbling $\approx$ 19.9 years (most realistic value)

Pioneer spacecraft with unburned TE 364, booms folded, end-on $\approx$ 15.3 years (minimum value)

Pioneer spacecraft with unburned TE 364, booms folded, crosswise $\approx$23.5 years (maximum value)

Similar calculations for the above configurations with booms unfolded were not made since the effects of unfolded booms on orbital lifetime would be relatively small.

There is a possibility of the Pioneer spacecraft with TE 364 motor (burned) entering into an orbit corresponding to the nominal Centaur MECO abort. This can happen if the spacecraft and TE 364 tumble during TE 364 burn such that the net ΔV from the TE 364 burn is zero. Therefore, similar orbital lifetime calculations for the Pioneer spacecraft with TE 364 motor (burned) were made. The results are:

Pioneer spacecraft with burned TE 364, booms folded, randomly tumbling $\approx$4.9 years (most realistic value)

Pioneer spacecraft with burned TE 364, booms folded, end-on $\approx$3.8 years (minimum value)

Pioneer spacecraft with burned TE 364, booms folded, crosswise $\approx$5.8 years (maximum value)

General Dynamics has computed an orbital lifetime for this abort of 3.5 years for the Centaur - TE 364 - spacecraft tumbling.

The probability of aborts resulting in the initial orbit used for the analyses, according to preliminary results from General Dynamics, is approximately 0.8×10^{-3}. A memorandum is being written to document the above orbital lifetime analysis.

<u>Orbital Decay Reentry Analysis</u> (W. H. McCulloch)

The two-dimensional thermal model of the Pioneer heat source previously developed was modified to include updated heating rates for orbital decay. The capsule model includes a copper-zirconia thermal switch, helium gaps inside the clad, and air gaps outside the clad.

The present analysis utilizes the TTB-13 code to compute the trajectory from 400,000 feet altitude to impact, including free molecule, transition, and continuum flow regimes. The temperatures of several locations in the heat source are shown in the column I of Table II. Corrections were calculated which modified the reference heating rates to include the effects of blockage, chemical reactions, and hot wall. The data in column II of Table II were obtained from the model using these corrected heating rates. In order to place a lower limit on the predicted impact temperatures, the corrections due to blockage and chemical reactions were omitted after the heat source passed Mach 2. These results are given in column III of Table II.

TABLE II

Calculated Peak and Impact Temperatures of the Pioneer Heat Source

	I	II	III
Peak Temperatures (°F)			
External POCO	4212	4069	4069
Internal POCO	4107	3978	3978
External Switch	4048	3919	3919
Internal Switch	3475	3384	3384
Pt-Rh Clad	3286	3198	3198
T-111 Strength Member	3213	3133	3133
Ta-W Liner	3177	3103	3103
Impact Temperatures (°F)			
External POCO	1603	1713	1478
Internal POCO	1629	1733	1507
External Switch	1803	1881	1741
Internal Switch	2408	2406	2299
Pt-Rh Clad	2675	2647	2547
T-111 Strength Member	2739	2706	2634
Ta-W Liner	2807	2770	2705

The data show that correcting for the blockage, chemical reactions, and hot wall lowers the peak temperatures somewhat but has only a small effect on the impact temperatures of the internal capsule parts. Neglecting the blockage and chemical reactions corrections after Mach 2 predicted internal impact temperatures which are less than 100°F lower. The temperatures in column II are regarded as the best prediction presently available.

Development work is continuing on a three-dimensional thermal model of the Pioneer capsule.

ISOTOPE BRAYTON SYSTEM

Isotope Brayton Safety Feasibility Study (IBSFS) (L. A. Hanchey)

The IBSFS is to provide the AEC with an in-depth risk assessment of the Isotope Brayton System as proposed for use on the Space Station. It is intended that safety problems be identified and recommendations relative to this application be included in the study. The IBSFS is directed by SNS and managed by AEC through Sandia Laboratories using a Task Force type approach. The Task Force includes members from NASA (OART, LeRC, MSFC, MSC, ARC), LASL, NUS, SNS, and Sandia.

An interim briefing for M. Klein, Director SNS, was presented on July 22, 1970, at AEC Headquarters. The input data for the study were reviewed, and additional input data were identified for inclusion in the study. The briefing was well received by those in attendance, with only one additional requirement being placed on the Task Force. Mr. Klein requested that a chapter addressing the uncertainties associated with the data being presented be included in the report.

A review of a preliminary rough draft report by the Task Force was held at Sandia August 25-27, 1970. Numerous comments relative to additions, corrections, and deletions were received. These comments were incorporated into a revised draft of the report which was mailed to Task Force members on September 28, 1970. A Task Force meeting will be held October 6-7, 1970, to review the revised draft report.

The final briefing for Mr. Klein is presently planned for October 14, 1970.

Ascent Abort Reentries (D. E. Randall)

The envelope of initial reentry conditions (velocity and reentry angle) at 400,000 feet altitude resulting from a 20 second uncontrolled burn of the INT-21 launch vehicle was analyzed to define that condition which results in the maximum heating rate ascent abort reentry. The Isotope Reentry Vehicle (IRV) reentry trajectory was computed for that condition resulting in the maximum heating rate. This information was developed as an input to the IBSFS.

Reentry Heating (R. D. Klett)

Reference heating rates for free molecule flow and heating rate distributions for ablated and unablated configurations of the Isotope Brayton Heat Source (IBHS) in free molecule and continuum flow were developed for use in the IBHS feasibility study. Limits of the transition flow regime were also furnished.

Terminal Velocities (A. C. Bustamante)

A memorandum describing the procedures and analysis used in computing the terminal velocities for the IBHS, fuel capsule, and IRV was written.

Trajectory Analysis (A. C. Bustamante)

Initial conditions for fourteen launch abort trajectories were analyzed, and corresponding heat source reentry trajectories were computed. The trajectories resulting in the maximum instantaneous heating rate and maximum total heat input were defined and used for further thermal analyses on the heat source.

Abort Models (L. L. Keller)

Preliminary estimates were made of various explosive abort models (INT-21 launch abort and ascent abort; in-orbit explosive aborts of the Shuttle, crew/cargo modules, free-flying modules, attached modules, and on-board experiments; and Shuttle reentry) to support the IBHS feasibility study.

Probabilities (L. L. Keller)

Point estimates were made of the fragment hit probabilities and fuel release probabilities during launch, in-orbit, and recovery of the IRV.

Analytic Techniques (C. J. M. Northrup, Jr.)

The helium release for the IBHS was analyzed using the HELIUM computer code and the latest information on full size solid solution cermet (SSC) fuel disks. The analysis followed the fuel from fabrication through the initial fuel storage period, encapsulation, system storage, launch, normal operation, reentry, and postimpact behavior.

The fuel parameters were obtained from LASL. The initial calculations give a D-prime value for helium diffusion equal to:

$$D' = D/r^2 = 2.6 \times 10^{-9}/\text{sec at } 800^\circ\text{C}$$

for a full size puck where D = diffusion coefficient (cm^2/sec) and r = effective radius of the fuel (cm). This value was assumed to be a "steady state" coefficient, and the reduction in the steady state D-prime value relative to earlier samples was attributed to an increase in the effective radius of the full size puck over previous experimental specimens. Hence, the steady state coefficients used in HELIUM were

$$D' = 4.2 \times 10^{-9} \times e^{-1.1/RT} + 1.3 \times 10^{+6} \times e^{-86./RT}$$

and the transient values were

$$D' = 7.7 \times 10^{-7} \times e^{-1.28/RT} + 4.4 \times 10^{+2} \times e^{-36.3/RT}.$$

The computer code HELIUM attempts to account for the variation of the transient diffusion coefficient (TD) from the steady state diffusion coefficient (SSD) by changing the parameters from SSD to TD at either encapsulation (to release as much helium as is experimentally possible from the onset of encapsulation) or at the start of reentry (to achieve the maximum "reentry pressure pulse" effects that have been measured experimentally).

System Parameters -- The thermal histories analyzed in this study are given in Table III. This system was assumed to be encapsulated in one atmosphere of helium at 200°F and to have 139.6 cc of free gas volume.

TABLE III

Two Thermal Histories for IBHS

Time Period		Node 1 (200 watts fuel) (°F)	Node 2 (200 watts fuel) (°F)	
A. Fuel Storage	60 days	200	250	
System Encapsulation				
		Node 1 (133.3 watts fuel) (°F)	Node 2 (133.3 watts fuel) (°F)	Node 3 (133.4 watts fuel) (°F)
B. System Storage:	720 days	800	750	800
C. Launch Pad:	40 days	550	650	550
D. Normal Operation:	3650 days	2210	2255	2210
E. Reentry:	1) IBHS Orbital Decay - Side-on-Stable			
	2) IBHS Peak Heating Abort - Side-on-Stable			
F. Impact and Partial Burial in Estancia Playa Soil:	20 days	2233	2248	2233

The design and therefore the behavior of the vent has not been well defined at this time. The latest vent proposal incorporates a capillary tube with gas flow in the viscous range. If the limited number of experiments on capillary flow at TRW can be translated to an operational vent for the IBHS system and if this vent will leak gas at the rate it is generated in the fuel when the capsule pressure is 3.0 psi, and if the external environment is a vacuum and the vent is at 2220°F, then for moderate pressure differentials (maintaining the flow (F) in the viscous region) the flow will equal:

$$F = 2.62 \times 10^{-5} (P_i - P_o)^2 (293/T)^{1.63} \quad (1)$$

where P_i is the internal helium pressure (psi), P_o is the external helium pressure (psi), and T is the vent temperature in degrees Kelvin.

The behavior of this vent in the slip and turbulent flow regions is unknown. In addition, little is known about its behavior during opposed gas flows (for example, when the external atmosphere is air). A limited number of short term experiments by TRW in opposed gas flows suggest the capillary vent may appear essentially plugged for moderate internal helium pressures (~ 1 atm) and moderate external air pressures (~ 1 atm).

For this analysis Eq. (1) was assumed to be valid when the vent was not plugged. In the normal histories (Runs 5 through 8), the vent was assumed to be plugged on impact after reentry but to be unplugged at all other times. In an effort to account for the uncertainty in opposed gas flows and to determine the effects of early vent plugging, additional runs were made in which the vent was plugged whenever the capsule was on the ground. In these latter analyses the vent was unplugged only when the capsule was in space (Runs 1 through 4). Whenever the vent is unplugged, the external environment was assumed to be a vacuum. Table IV summarizes the eight system histories examined in this study.

TABLE IV

Summary of the IBHS Histories Analyzed by HELIUM

SYSTEM PARAMETERS	TIME PERIOD	1	2	3	4	5	6	7	8
DIFFUSION COEFFICIENT	A	SSD	SSD	SSD	SSD	SSD	SSD	SSD	SSD
	B	SSD	TD	SSD	TD	SSD	TD	SSD	TD
	C	SSD	TD	SSD	TD	SSD	TD	SSD	TD
	D	SSD	TD	SSD	TD	SSD	TD	SSD	TD
	E	TD	TD	TD	TD	TD	TD	TD	TD
	F	TD	TD	TD	TD	TD	TD	TD	TD
VENT OPERATION	B	VP	VP	VP	VP	VO	VO	VO	VO
	C	VP	VP	VP	VP	VO	VO	VO	VO
	D	VO	VO	VO	VO	VO	VO	VO	VO
	E	VO	VO	VO	VO	VO	VO	VO	VO
	F	VP	VP	VP	VP	VP	VP	VP	VP
REENTRY MODE	E	OD	OD	PH	PH	OD	OD	PH	PH

TD - Transient diffusion coefficients
SSD - Steady state diffusion coefficients
VP - Vent plugged
VO - Vent operational
PH - Peak heating - side-on-stable
OD - Orbital decay - side-on-stable

A = Fuel storage-60 days
B = System storage-720 days
C = Launch pad-40 days
D = Normal operation-3650 days
E = Reentry
F = Impact and post impact-20 days

Conclusions -- The capsule pressures versus time are shown in Figures 2 through 5. Runs 1 through 4 indicated that maximum pressures from 202 to 313 psi could occur at the end of system storage (Time period B) if the gas flow was severely suppressed or if the vent was mechanically plugged from the time of encapsulation. By experimentally determining the vent characteristics as functions of the external atmosphere, internal gas pressures, and vent temperature, and by specifying that the system have adequate monitoring before launch to insure adequate helium flow, the situations analyzed by Runs 1 through 4 can be avoided. Runs 5 through 8 indicate capsule pressures will not exceed 30 psi nor drop below 1 psi if the vent operates according to Eq. (1), and the systems history is as described above. Even during reentry, the peak capsule pressure did not exceed 7.0 psi.

On impact, the vent was assumed to be plugged and the capsule partially buried (2 inches) in Estancia Playa soil. Shortly after impact, the pressure rose to approximately 2.9 psi and then increased at approximately 0.73 psi per day.

These last four analyses suggest that a system designed around a capillary vent with flow properties described by Eq. (1) could perform satisfactorily with respect to internal capsule pressures. These analyses give added impetus to programs to develop such vents and to determine fundamental properties of vents.

IBHS Trajectory Analysis (M. D. Bennett/H. R. Spahr)

Two 6-degree-of-freedom trajectories for the IRV were completed. The initial trajectory conditions correspond to the maximum total integrated heating ascent to orbit abort, as defined by NASA/Ames. The two initial angular rates used corresponded to the roll rate required to gyroscopically stabilize the IRV backwards down to near peak heating and the pitch rate required to make the IRV tumble down to near peak heating.

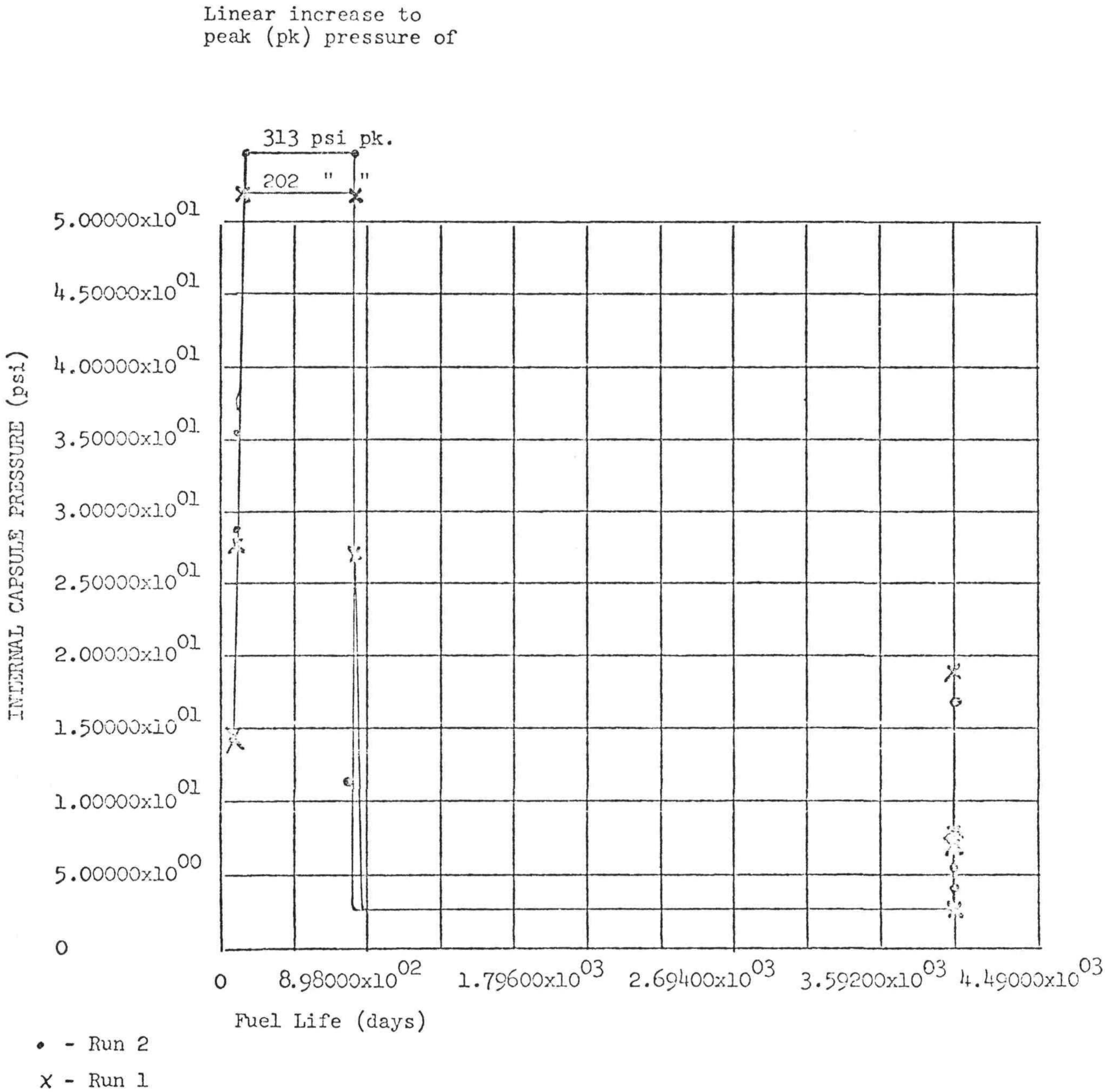

Figure 2. Internal capsule pressure is given as a function of fuel life for the orbital decay - side-on stable reentry. Capsule vent plugged before and after normal space operations.

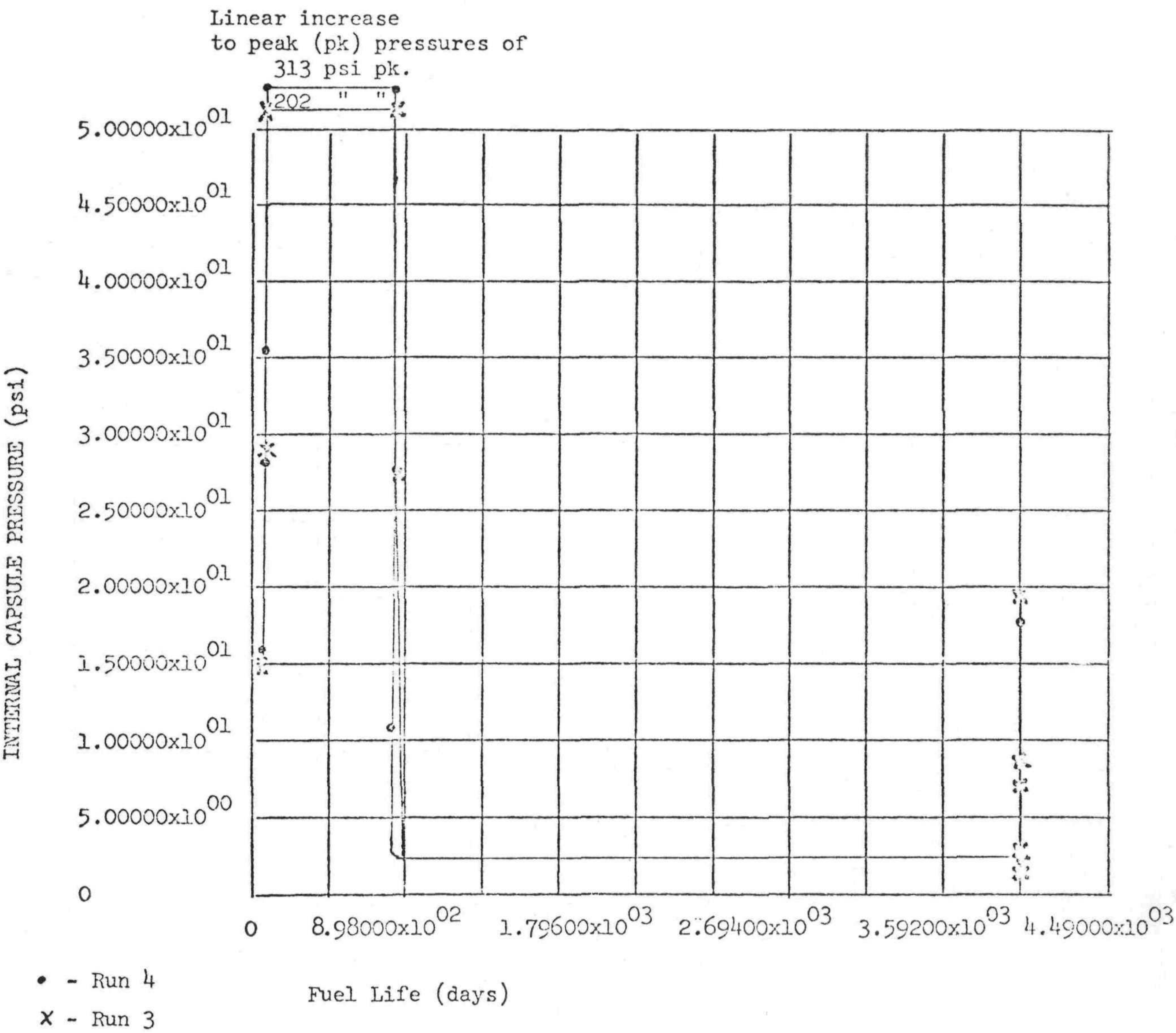

Figure 3. Internal capsule pressure is given as a function of fuel life for the peak heating side-on stable reentry. The capsule vent was plugged before and after normal space operations.

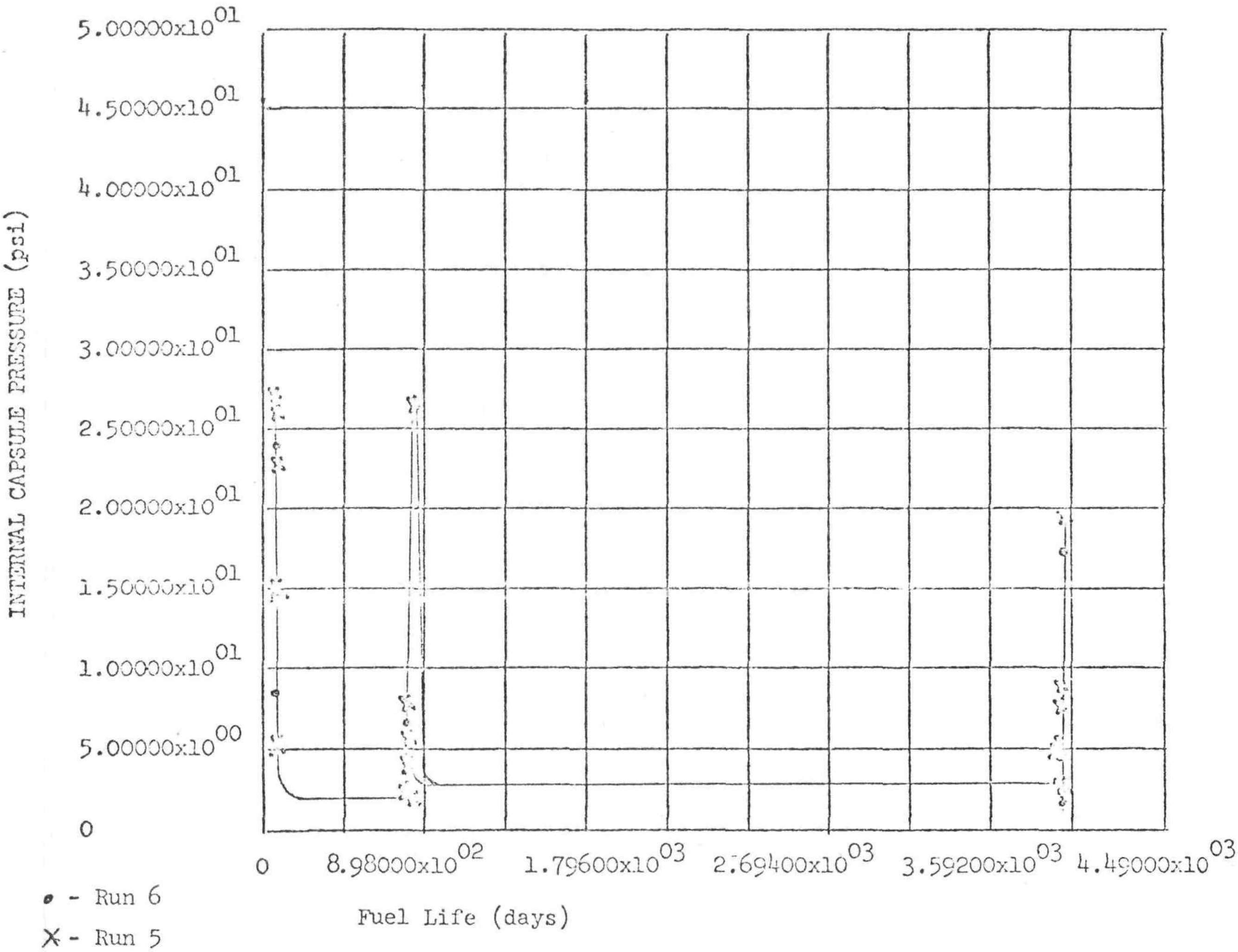

Figure 4. Internal capsule pressure is given as a function of fuel life for the orbital decay - side-on stable reentry. The capsule vent was plugged only after impact on reentry.

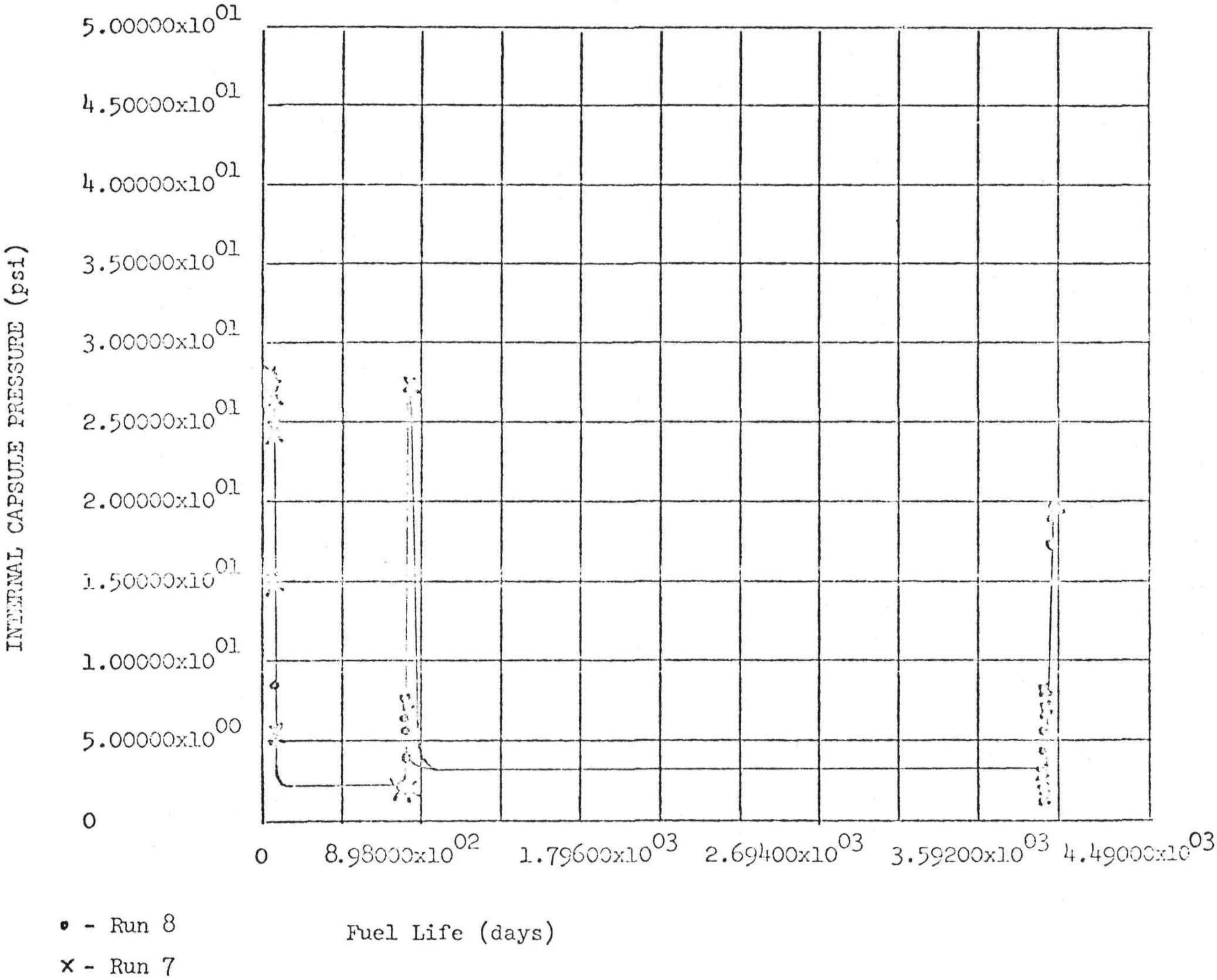

Figure 5. Internal capsule pressure is given as a function of fuel life for the peak heating - side-on reentry. The capsule vent was plugged only after impact on reentry.

The above trajectory conditions near peak heating were used to compute two 3-degree-of-freedom trajectories for the IBHS reentering crosswise, flat forward, unablated. These two trajectories bound the most probable IBHS reentry environment which would exist if the IBHS were to separate from the IRV during reentry.

A 3-degree-of-freedom trajectory was also computed for the IBHS reentering alone crosswise, flat forward, unablated, for the maximum total integrated heating ascent to orbit abort. This trajectory was used as a reference to define the effects on the aerodynamic heating to the IBHS for the IBHS remaining on the IRV down to peak heating and for different initial angular rates of the IRV.

IBHS/IRV Heating Data (H. R. Spahr/S. McAlees)

Heating rate data (on IBM cards) were received from NASA/Ames for the center and edge of the IRV base for two trajectories. One trajectory was a zero degree angle of attack IRV reentry. The other trajectory was for the tumbling IRV. Initial trajectory conditions corresponded to the worst total integrated heating ascent to orbit abort, as defined by NASA/Ames. These data were listed and reviewed.

DART

LASL Dart Minithruster Reentry Tests (Nandall/Deveney)

Seven test specimens of the Dart Minithruster heat source were subjected to an orbital decay reentry simulation in the Sandia HEAT Facility. Six were run in the side-on-stable orientation, and one was run end-on. All units survived the test satisfactorily. Repeatability of the ablation mass loss was very good.

SAFETY TECHNOLOGY

ADVANCED FUELS SAFETY

Reentry Ablation Testing in a Hyperthermal Arc Tunnel
(I. B. White/K. L. Romine)

The new 40 kW hyperthermal arc tunnel was installed at Sandia. The generator has been operated approximately thirty times; however, it has not yet been operated at its maximum design level. The tunnel is designed to produce stagnation enthalpies ranging up to 15,000 Btu/lb and model pressures ranging up to 2 atmospheres on specimens of 1/2 inch diameter or less.

Modifications to the water, gas, and calorimeter systems are being made to optimize the entire operation. When these modifications are complete, the generator will be calibrated to reproduce several specific simulated reentry heat fluxes and pressures. Figure 6 shows the arc tunnel with viewing and camera ports, heat exchanger, absolute filter, water tanks, and water pumps. Figure 7 shows the 40 kW generator and arc tunnel. Figure 8 shows the console with power controls, gas and pressure sensors, voltage and current meters, water flow meter, and recorders.

The new 40 kW hyperthermal arc tunnel for testing nonradioactive specimens was received, and is being set up in parallel with the system described above. A single console is designed to control both arc tunnels.

Isotope Fuels Impact Facility (W. J. Dalby)

To provide an additional safety margin, the vertical airgun facility designed for impacting radioisotope fuel and fuel simulants* will be placed in a partially buried steel containment vessel (Figure 9).

*SC-PR-70-881, Sandia Laboratories Quarterly Report Aerospace Nuclear Safety Program October 1 through December 31, 1969, Aerospace Nuclear Safety Department, Sandia Laboratories, Albuquerque, New Mexico, January 1970.

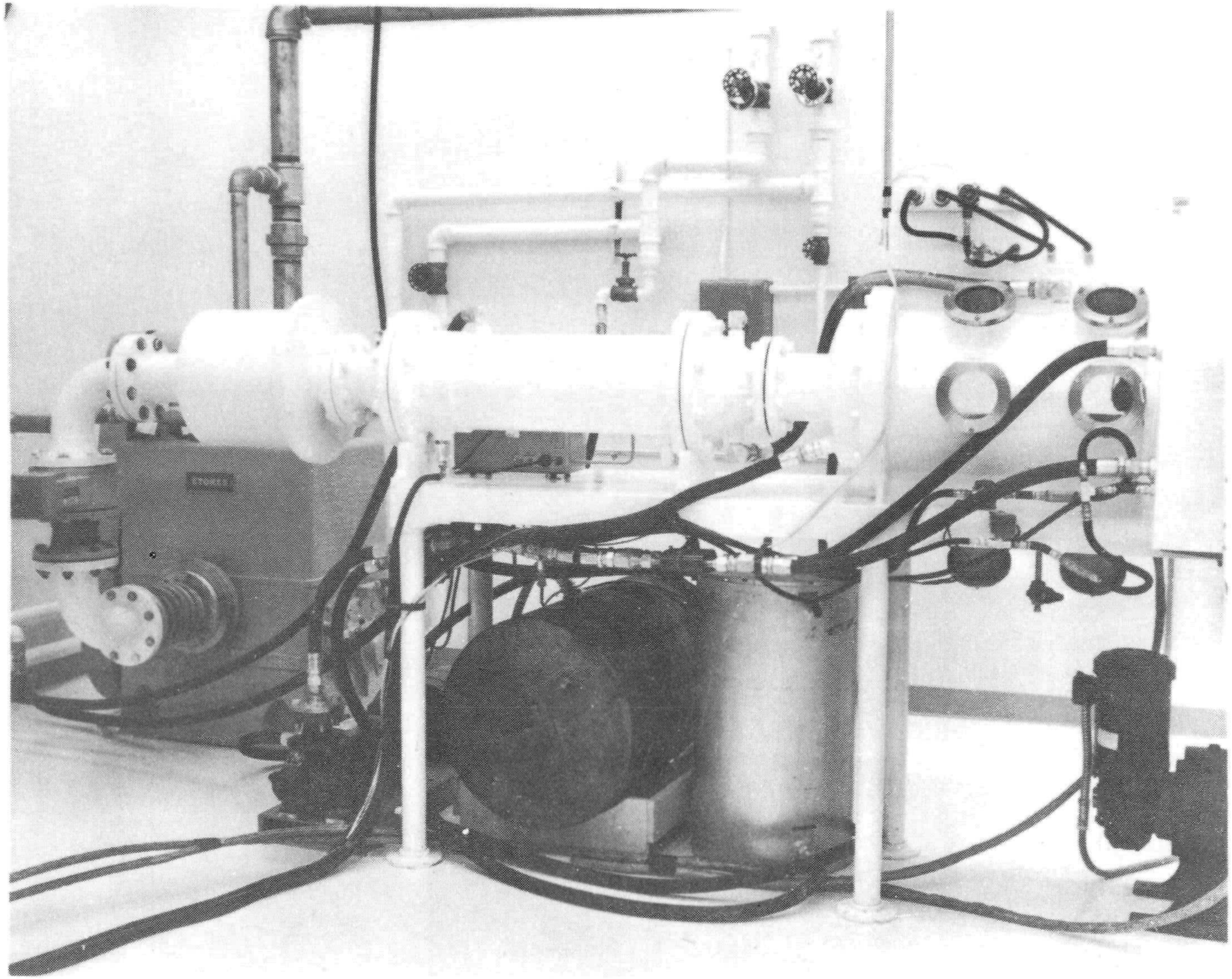

Figure 6. Arc tunnel setup

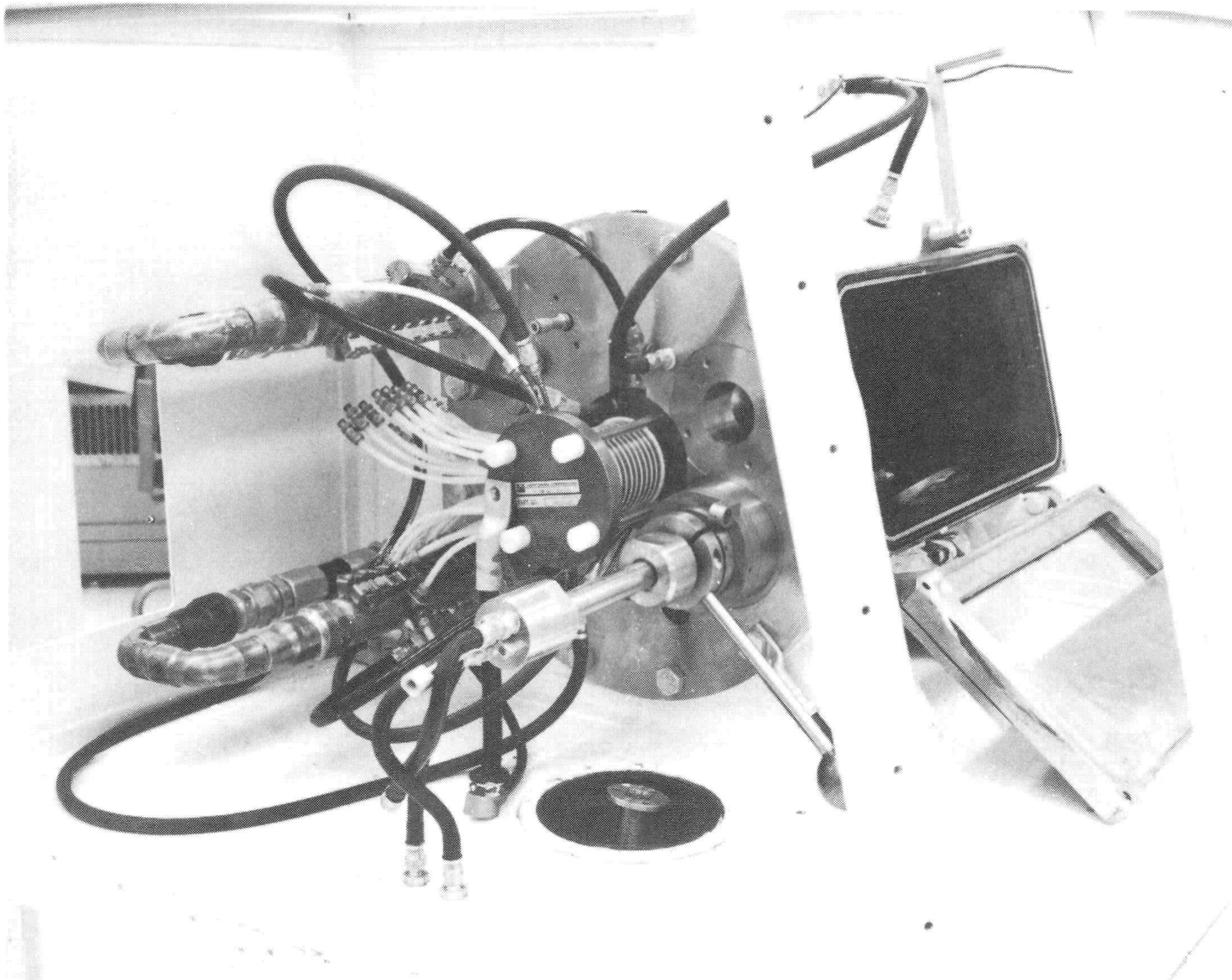

Figure 7. 40 kW generator and arc tunnel

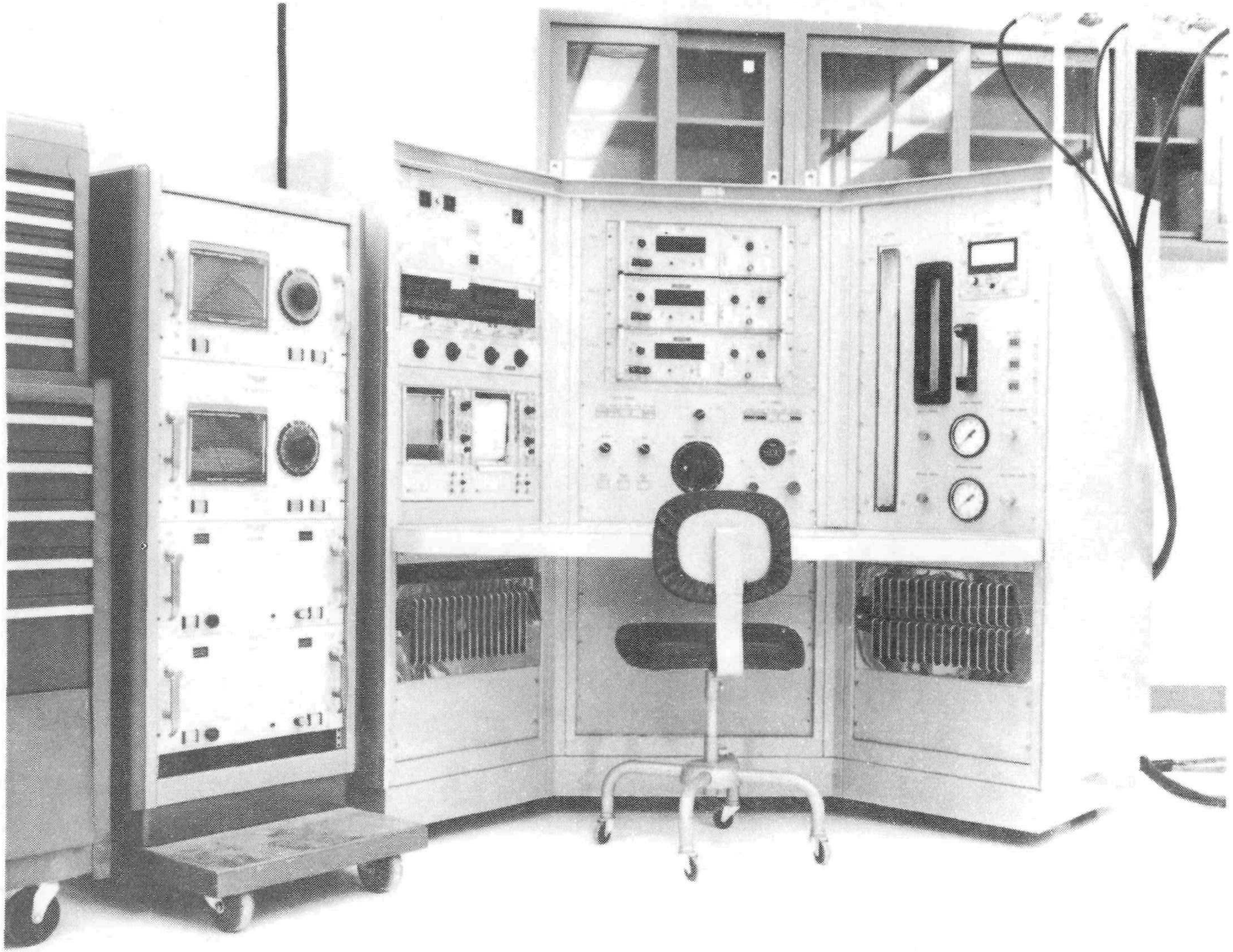

Figure 8. Arc tunnel console

The vessel was installed, backfilling was completed, and the concrete pad was poured. The blower, filters, valves, stairs for the chamber, hoist, and the beam and columns for the hoist are presently on hand and will be installed as the work can be scheduled.

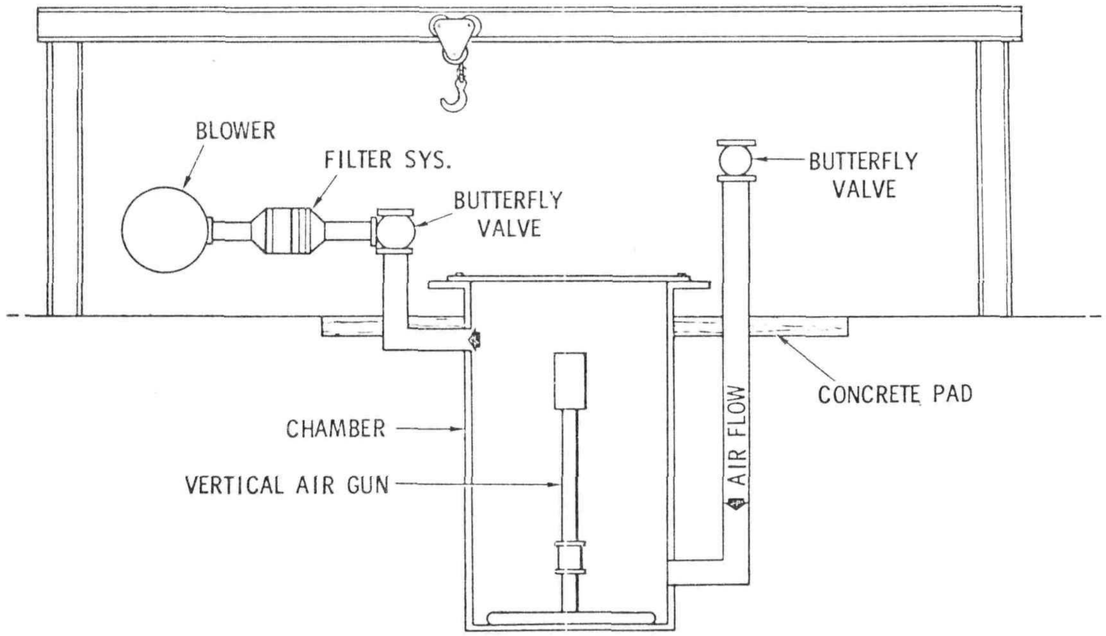

Figure 9. Isotope fuel impact facility

Fuels Impact (W. J. Dalby)

Six additional impacts of single full scale solid solution cermet simulant (SSCS) disks were completed as part of the experiment designed to investigate the main effects and two factor interactions of temperature, velocity, and disk attitude.* Impact conditions were: ~270 and ~850°F, ~140 and ~425 fps, and 0° (flat) and 45° attitudes.

Five additional disks were encapsulated, and two more are presently available at Sandia for encapsulation. Impacts of these seven disks will complete the 270° and 850°F portions of the referenced test program.

*SC-PR-70-222, Sandia Laboratories Quarterly Report Aerospace Nuclear Safety Program January 1 through March 31, 1970, Aerospace Nuclear Safety Department, Sandia Laboratories, Albuquerque, New Mexico, April 1970.

To investigate the effect of varying molybdenum content on the particle size distributions resulting from impact, five full scale SSCS disks were impacted singly at ~850°F, 320 fps, and 0° disk attitude. The disks (90, 86, 75, 65, and 50 percent ThO_2) were furnished by LASL. They were encapsulated and impacted at Sandia. The capsules were sent to LASL where they will be opened and the particle size analyses performed.

Track Side Attempt to Detect Airborne Thoria (D. J. Sasmor)

The fuel simulant (SSCS) in the impact test capsules contains thoria (ThO_2) as a major constituent. Since this material is radioactive (1.11×10^{-7} Ci/g), it was considered possible to detect fine particulate (1) if the capsule breached on impact and released fine material, (2) if the samples could be obtained under the dynamic test conditions, and (3) if the method chosen would not interfere with the tests and test schedules. Under the prescribed conditions, it was decided to use passive "fallout" plates (12 x 12 inch glass with the surface covered with double adhesive pressure sensitive tape). These were placed along both sides of the sled track in a staggered array, beginning 10 feet past the impact point and extending 200 to 250 feet down track. A fresh set of plates was placed track side for each impact test. If, from visual examination of the impacted capsule, it appeared that the capsules were breached, the plates were bagged and delivered to the Sandia Health Physics Laboratory for analyses.

No thoria was detected on any of the fallout plates, although several of the capsules did breach, and the swipes of the surface of one, T-33, gave alpha counts of the order of 12 CPM above background. The absence of detectable quantities of thoria on the fallout plates should not and may not be considered as evidence that there were no airborne fines. While it may be possible that this is a correct conclusion, there is no additional supportive evidence and, at the same time, there are many "holes" in the sampling technique (i.e., total area coverage was only 12 ft^2) and the low level of activity of the thoria was further complicated by the presence of the molybdenum.

Alpha Particle Irradiation of Molybdenum (C. J. M. Northrup, Jr./ R. P. Wemple/G. J. Thomas/C. R. Hill)

Alpha particle irradiation of a metal can significantly change its physical properties. After six months exposure, the molybdenum matrix of a cermet fuel form can receive alpha doses as high as 0.1 atomic percent. The effects of these high alpha doses on molybdenum are just beginning to be understood, and more detailed studies are being carried out.

The work during this quarter was concentrated on the low energy implantation technique. Concurrent microscopic observation and helium release experiments have yielded several interesting results.

Electron Microscopy -- An implanted concentration of 1.0 atomic percent was taken as standard to eliminate dose effects. Dose effects will be studied as an independent parameter. Anneals to various temperatures for fixed times (15 min) were made with the following results.

1. High densities of bubbles were found after annealing to 600°C or greater. Minimum detectable bubble size is 15 Å diameter.

2. Annealing to higher temperatures produced larger bubbles in reduced concentrations. Size distributions were determined at various temperatures and show that the smaller bubbles agglomerate to form larger ones. The larger the bubble, the more immobile it becomes.

3. Above 700°C the bubbles appear distinctively polygonal with the faces parallel to (110) planes.

4. Considerable dislocation-bubble interaction occurs, which is not completely understood as yet. However, it would appear that considerable dislocation pinning occurs.

5. High densities of bubbles are observed on grain boundaries and on twin planes. It is possible that the highly localized bubble concentrations could considerably change the intergranular bonding and alter the fracture properties of the material. In multiphase material one would expect the bubbles to occur at the interfaces.

Gas Release Measurements -- The release of helium from the surface of the low energy implantation specimens was observed at temperatures as low as 150°C. Increasing the sample temperature changes the nature of the release from a continuous emission to a "burst" type release characterized by a rapid series of gas pulses. The burst type release was detected at temperatures as low as 300°C. Short term anneals at 600°C released only a fraction of the implanted gas, and 20 minute anneals at 1500°C were required to stabilize the helium release.

In summary, it was shown that long term alpha irradiation of molybdenum can produce changes that can be expected to alter the fracture properties of the molybdenum and could lead to dimensional changes.

FLINTNOSE-1

Aerodynamic Analysis (A. C. Bustamante)

Ballistic parameters were determined for the five different heat sources on the FLINTNOSE-1 payload. Free molecular and continuum values (Table V) were determined, as well as the variation of the parameter values throughout the transitional region. All the parameters were based on three types of motion; end-on, side-on, and end-over-end tumbling.

Thermal Analysis (A. C. Bustamante)

The thermal analysis of the instrumented heat source was updated to reflect the latest data on the thermal conductivity of the fibrous carbon insulator. The results show that the internal temperatures are slightly higher ($\approx$10 percent). Temperatures measured by the instrumented heat source when subjected to a heating rate of 1.3 times the expected heating rate were compared to temperatures that were obtained for the expected heating rate. The results are shown in Figures 10 and 11. For node 1, the temperature corresponding to the higher heating rate is approximately 4025°F compared to a temperature of 3300°F for the lower heating rate. This comparison was made in order to obtain a realistic indication of the temperature range needed for the thermocouples which will be installed in the instrumented heat source.

TABLE V

Continuum and Free Molecule Ballistic Parameters

Unit Number		C_D End-on	C_D Side-on	C_D (EOE)Tumble	W/C_DA End-on	W/C_DA Side-on	W/C_DA (EOE)Tumble
1 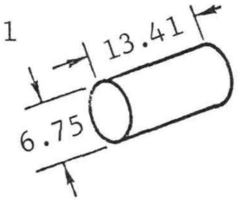	Free molecule	0.93	2.12	1.29	63.11	27.6	45.5
	continuum	0.65	1.18	0.78	90.31	49.75	75.0
2 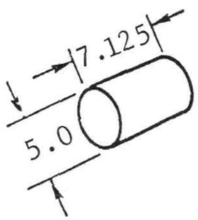	Free molecule	0.982	2.0	1.898	57.84	28.34	29.8
	continuum	0.823	1.18	0.850	68.8	48.03	66.7
3 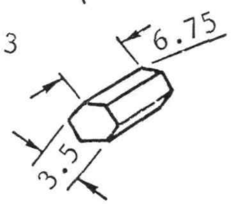	Free molecule	0.9699	2.54	1.49	67.58	25.81	43.9
	continuum	0.81	1.37	0.93	80.93	47.8	70.5
4 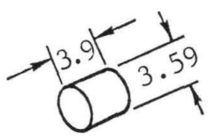	Free molecule	1.58	2.12	1.57	41.69	31.0	41.9
	continuum	1.21	1.18	1.02	54.4	55.83	64.6
5 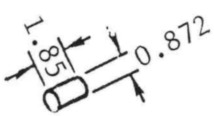	Free molecule	0.981	2.12	1.31	10.92	5.05	8.17
	continuum	0.71	1.18	0.80	15.07	9.07	13.4

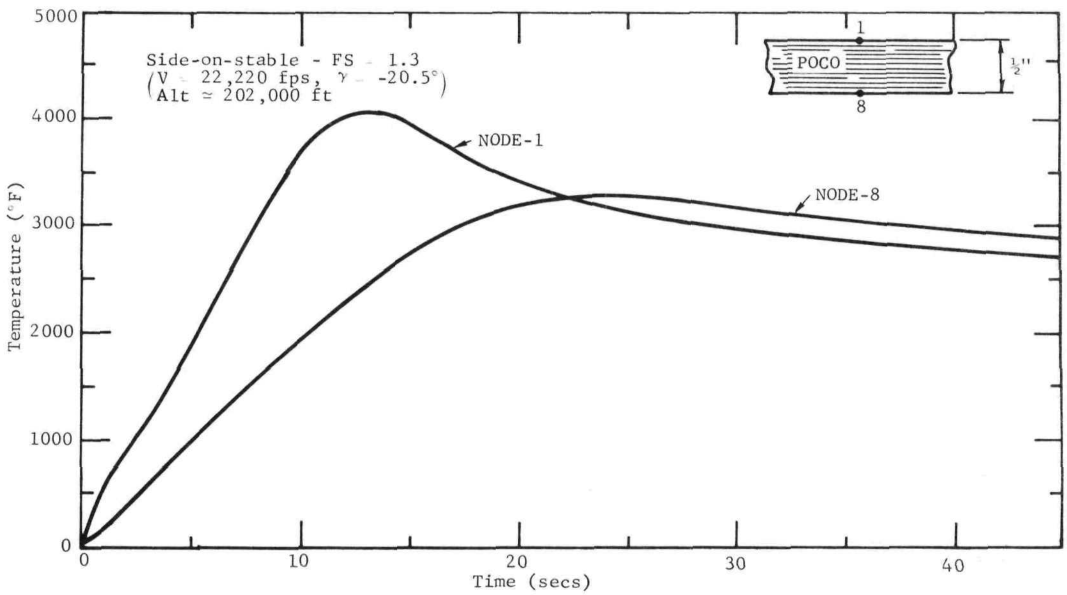

Figure 10. FLINTNOSE 1 -- temperature vs time

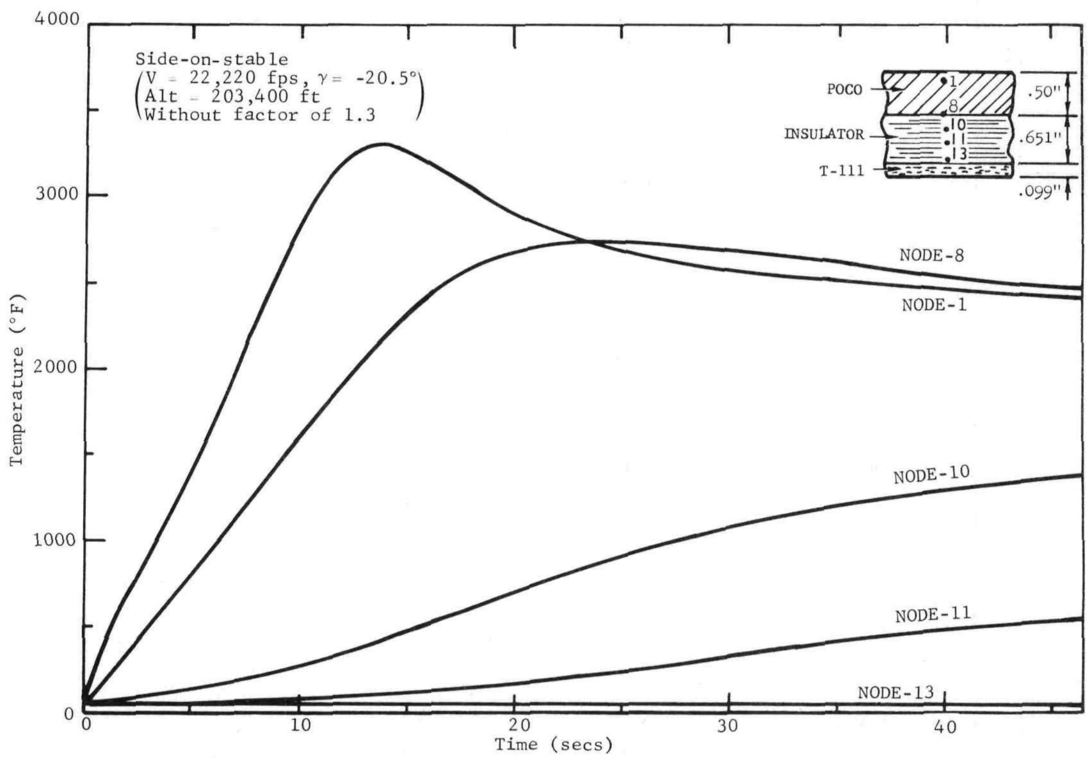

Figure 11. FLINTNOSE-1 -- temperature vs time

Trajectory Analysis (A. C. Bustamante)

New trajectory conditions for the FLINTNOSE-1 were determined by ARC and are as follows:

Release Altitude = 293,000 ft
Velocity at Release = 21,600 fps
Reentry Angle at Release = -19.9 degrees.

Trajectories reflecting these new conditions were computed. They show a reduction in peak heating rate of 10 percent and an increase in integrated heat input of 10 percent from the previous Athena H trajectory conditions.

Radiological Safety Analysis Summary Report (A. C. Bustamante/ M. Parsont)

A Safety Analysis Summary Report was prepared which provides data regarding the quantities, types, and locations of radionuclides for the FLINTNOSE-1 payload (Figure 12). Described in this report are the launch vehicle, its payload, and associated radioisotopic devices. The radiation activity level for each source is presented, as well as the total intensity level (Table VI). The flight mission (environment) is described along with the safety criteria and responsibilities for postflight recovery. The safety significance of allowable doses described, and the computed dose rates presented (Figure 13). The safety implications, consequences, and conclusions are summarized. This report was submitted to SAMSO as part of the required documentation for FLINTNOSE-1.

Payload Configuration/Objective Agreement (PC/OA) A. C. Bustamante/J. E. Deveney)

The physical prospect of data, weights, moments of inertia, and centers-of-gravity were determined for the various heat sources (Table VII). These data served as input for the PC/OA document. Also supplied as input for the PC/OA were the ballistic coefficients (W/C_DA) as a function of Mach number and altitude. In addition, the maximum and minimum ballistic coefficients were determined for use in ARC's dispersion analysis.

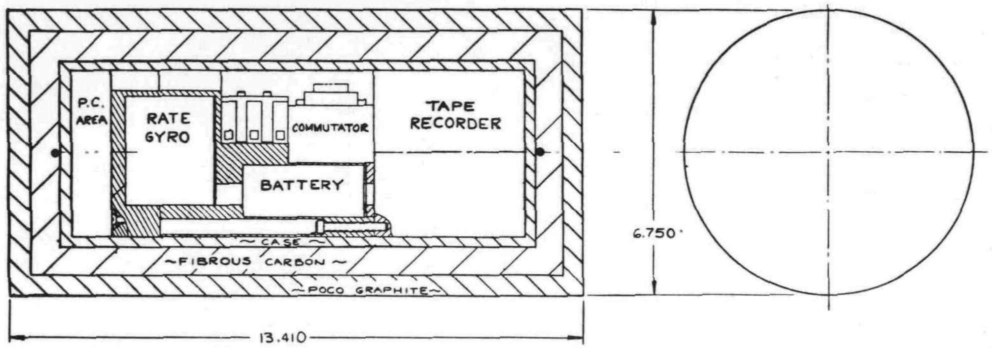

① INSTRUMENT UNIT (MOTION & THERMAL)

• Denotes tantalum wire approximately 50 mCi per wire.
(Wire approximately 1/2 to 1 inch long, 20 to 30 mils in diameter.)

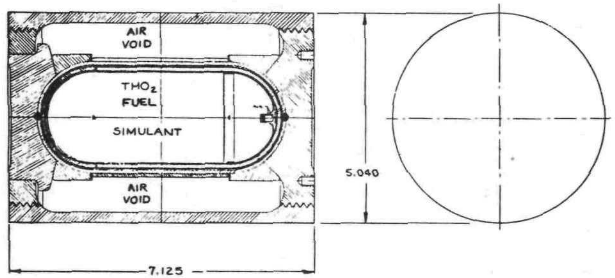

② TRANSIT HEAT SOURCE

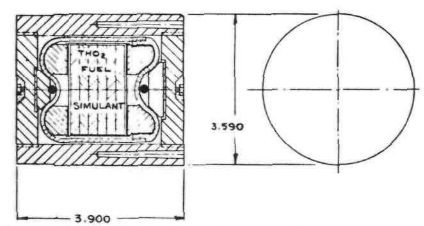

④ HEAT SOURCE, DART THRUSTER (LASL)

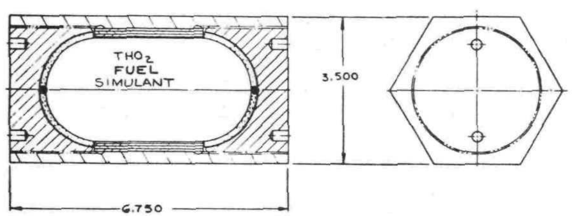

③ PIONEER HEAT SOURCE

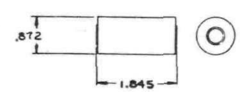

ACTUAL SIZE

⑤ PIONEER HEATER
⑥ IDENTICALLY EQUAL TO ⑤

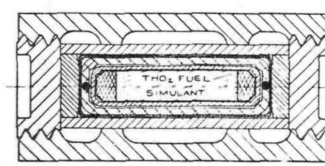

SCALE: 4/1

Figure 12. Location of radionuclides in FLINTNOSE-1 payload

TABLE VI

Radiation Levels for Various FLINTNOSE-1 Heat Sources

Heat Source Configuration	Activity[1] Level Inside Heat Source From			Activity Level Outside Heat Source From		
	^{182}Ta (mCi)[2]	Thorium Simulant (mCi)	Total (mCi)	^{182}Ta (mCi)	Thorium Simulant (mCi)	Total (mCi)
#1 Instrumented	121	--	121	100	--	100
#2 Transit	118	0.232	118.23	100	0.162	100.16
#3 Pioneer	118	0.176	118.18	100	0.123	100.12
#4 Dart	118	0.094	118.09	100	0.065	100.07
#5 Pioneer Heater	109	0.00028	109.	100	0.000196	100.
#6 Pioneer Heater	109	0.00028	109.	100	0.000196	100.
		Grand Total	693.5 millicuries		Grand Total	600.35
			≈ 694			≈ 601

(1) *This is the activity level presence on the flight date.*

(2) mCi = millicuries.

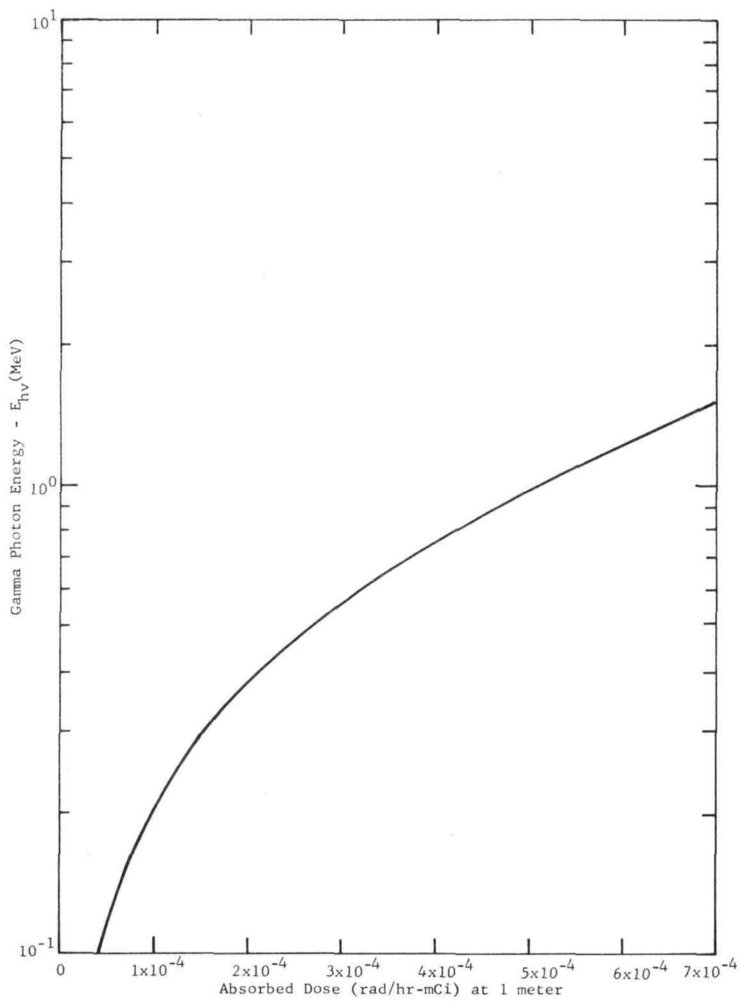

Figure 13.

Gamma photon energy and absorbed dose in tissue at 1 meter

TABLE VII
Physical Property Data for FLINTNOSE-1 Payload

Unit Number	Weight (lbs.)	Center of Gravity (inches)	Imbalance Dynamic (lb-in.^{2})	Moments of Inertia* (lb-in.^{2}) Roll	Pitch	Yaw
1 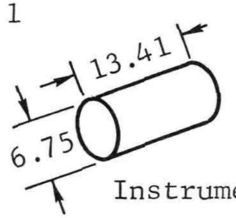 Instrumented	37	0.01 Y&Z 0.07 X	0.0259	175	540	540
2 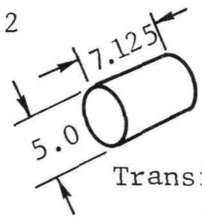 Transit	13	geometric center	0.008	27	62	62
3 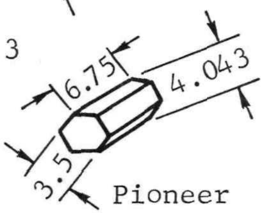 Pioneer	11	geometric center	0.004	12.6	29.4	29.4
4 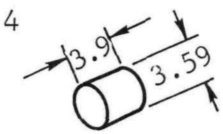 DART	5	geometric center	0.0016	5.9	6.84	6.84
5&6 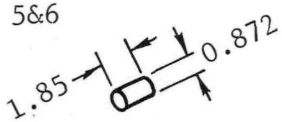 Pioneer Heater	0.12	geometric center	0.158-6	0.0114	0.04	0.04

*NOTE: Moments of inertia are about each unit's CG

Payload Interface Studies (A. C. Bustamante/R. E. D. Stewart)

Preliminary layout drawings for the Sandia payload were recieved from Atlantic Research (ARC). These drawings were examined, and various improvements were suggested to Atlantic Research. An approximate analysis was conducted to determine the stresses imparted to the graphite shells of the various payloads due to the loading by the retaining strap. Results indicate that a 2000 pound strap force is marginal. The possibility of reducing the originally suggested 2000 pound strap force is being considered by ARC.

Miscellaneous Studies (A. C. Bustamante)

The effect of radiation from the radioactive source (^{182}Ta) on the various instrumentation components was determined analytically. Tests will be conducted to verify the analysis.

Mockup of the instrumented heat source is almost complete except for the wiring. Most of the components for the instrumented unit have been received. The commutator and the thermocouples still remain to be obtained.

A payload coordination meeting was held with Atlantic Research and SAMSO on August 19, 1970. Also represented was Lincoln Laboratories, who will have a piggyback payload on the second Athena H R&D flight. Items discussed were: the piggyback payload adapter, the new release conditions for the payloads, and the various upcoming milestone dates. From the above meeting, it appears that to meet the schedule, close coordination and timing will be required among all the groups involved in Athena H R&D flight No. 2.

COMPUTER CODES

Radiant Heating Code (D. W. Larson/ H. R. Spahr)

Computer code CALLIS, which computes the stagnation point radiative aerodynamic heating to blunt objects, was received from NASA/Langley. The necessary changes to make this computer code run on the Sandia computers were made.

The results of the sample run were reproduced within a few percent. The differences in operating systems which result in the code terminating the iteration procedure slightly earlier on the Sandia computers will be defined, and any necessary changes will be made to the computer code.

GE Arbitrary Body Code (H. R. Spahr)

The GE Arbitrary Body Computer Code calculates the free-molecule and continuum hypersonic aerodynamic coefficients of complex configurations, including shielding. Conversion of this code from the Univac 1108 to the CDC 6600 computer is approximately 50 percent complete.

Douglas Arbitrary Body Code (H. R. Spahr)

The Douglas Arbitrary Body Code calculates the hypersonic aerodynamic coefficients of complex configurations using several theoretical methods. A source deck and documentation for the graphics terminal version of this code were received from NASA/Langley and are being reviewed by Sandia.

The Air Force Wright-Patterson Flight Dynamics Laboratory, at their request, is being kept informed on the evaluation of the compatibility of the NASA graphics routines with the Sandia graphics routines and graphics terminal equipment.

CDC 3600 Computer Codes (H. R. Spahr)

All computer codes maintained and used by the Reentry and Space Sciences Division of Sandia are being reviewed to define the codes which are operational only on the CDC 3600 computer. A priority list and a schedule for conversion of these codes to other computers are being prepared because the CDC 3600 computer is scheduled for release November 1, 1970.

HRS017 Computer Code (H. R. Spahr)

Computer code HRS017 calculates the trajectory and reentry environment for nuclear systems decaying from highly elliptical orbits. Complete documentation, a FORTRAN source deck, sample input, and sample output of this code were transmitted to Isotopes, Inc., at their request.

This computer code is now available through the Computer Software Management and Information Center (COSMIC), and it is listed in their current listing of computer codes.

DISTRIBUTION:

TID-4500 (56th Ed.) UC-36 (150)

U. S. Atomic Energy Commission (5)
Division of Space Nuclear Systems
Space Electric Power Office
Washington, D.C. 20545
Attn: G. A. Newby
Assistant Director
G. P. Dix, Chief
Safety Branch
H. Jaffe, Chief
Isotope Power Sys. Branch
J. A. Powers, Chief
Isotopes Fuels and Matls. Br.
C. E. Johnson, Chief
Reactor Power Sys. Branch

U. S. Atomic Energy Commission
Space Nuclear Propulsion Office
Washington, D.C. 20545
Attn: R. S. Decker, Jr., Chief
Safety Branch

U. S. Atomic Energy Commission
Division of Isotope Development
Washington, D.C. 20545

U. S. Atomic Energy Commission (2)
Director of Regulation
Washington, D.C. 20545
Attn: C. K. Beck
Deputy Director
R. W. Klecker
Div. of Reactor Licensing

U. S. Atomic Energy Commission (2)
Division of Biology and Medicine
Washington, D.C. 20545
Attn: J. Z. Holland
Fallout Studies Branch
H. D. Bruner, Asst. Dir.
Medical and Health Research

U. S. Atomic Energy Commission
Space Nuclear Propulsion Office
Albuquerque Extension
Albuquerque Operations Office
P. O. Box 5400
Albuquerque, New Mexico 87115
Attn: H. P. Smith

U. S. Atomic Energy Commission (2)
Albuquerque Operations Office
P. O. Box 5400
Albuquerque, New Mexico 87115
Attn: V. V. Berniklav, Director
Space and Special
Projects Division
For: J. Nicks
J. F. Burke, Director
Operational Safety Div.

AEC Site Representative
National Aeronautics and Space Adm.
Manned Spacecraft Center
Houston, Texas 77058
Attn: W. C. Remini
Bldg. 16, Code ZS-5

Deputy I. G. for Insp. & Safety
USAF
Directorate of Nuclear Safety
Nuclear Power Division
Kirtland Air Force Base
New Mexico 87117

Jet Propulsion Laboratory
California Institute of Technology
4800 Oak Grove Drive
Pasadena, California 91103
Attn: A. L. Klascius
Radiation Health and
Safety

Los Alamos Scientific Laboratory (5)
P. O. Box 1663
Los Alamos, New Mexico 87544
Attn: Dr. L. D. P. King
Dr. Wright Langham
C. F. Metz, CMB-1
F. W. Schonfeld, CMF-5
J. A. Leary, CMB-11

Monsanto Research Corporation
Mound Laboratory
P. O. Box 32
Miamisburg, Ohio 45342
Attn: G. R. Grove

DISTRIBUTION (cont):

Thomas B. Kerr
Code RNS
National Aeronautics and Space Adm.
Washington, D.C. 20545

Mr. Glenn Goodwin
National Aeronautics and Space Adm.
Ames Research Center
N-200-4
Moffett Field, California 94035

National Aeronautics and Space Adm.
Goddard Space Flight Center
Glenn Dale Road
Greenbelt, Maryland 20771
Attn: A. W. Fihelly
Nimbus Project

Naval Facilities Engineering Com.
Dept. of the Navy, Code 042
Washington, D.C. 20390

Space Nuclear Propulsion Office
Lewis Research Center
21000 Brookpark Road
Cleveland, Ohio 44135
Attn: L. Nichols

Mr. George Mandel
Information Specialist
Aerospace Safety Research and
Data Institute
NASA Lewis Research Center
21000 Brookpark Road
Cleveland, Ohio 44135

Union Carbide Corporation (2)
Nuclear Division
P. O. Box X
Oak Ridge, Tennessee 37831
Attn: R. A. Robinson
Isotope Development Center
B. R. Fish
Health Physics Division

U. S. Public Health Service
Nat. Ctr. for Radiological Health
1901 Chapman Avenue
Rockville, Maryland 20852
Attn: Nuclear Facilities Section

D. B. Shuster, 1200
J. R. Holland, 5321
C. F. Bild, 7500
G. A. Fowler, 9000
J. R. Banister, 9150
R. C. Maydew, 9320
L. A. Hopkins, Jr., 9500
A. J. Clark, Jr., 9510
S. L. Jeffers, 9512
ARPIC, 9512 (2)
S. McAlees, Jr., 9513
G. J. Hildebrandt, 9520
G. J. Hildebrandt, 9521 (Actg)
J. Jacobs, 9522
Library Division, 8232 (5)
Central Files, 3422-1 (15)
L. C. Baldwin, 3412
L. L. Alpaugh, 3412
G. C. McDonald, 3416 (3)
Attn: Miss P. R. Swartz